

START-TO-END SIMULATIONS FOR IR/THZ UNDULATOR RADIATION AT PITZ

P. Boonpornprasert*, M. Khojoyan, M. Krasilnikov, F. Stephan, DESY, Zeuthen, Germany
B. Marchetti, E. Schneidmiller, M. Yurkov, DESY, Hamburg, Germany
S. Rimjaem, Chiang Mai University, Chiang Mai, Thailand

Abstract

High brightness electron sources for modern linac-based Free-Electron Lasers (FELs) have been characterized and optimized at the Photo Injector Test facility at DESY, Zeuthen site (PITZ). Since the time structure of the electron bunches at PITZ is identical to those at the European XFEL, the PITZ accelerator is being considered as a proper machine for the development of an IR/THz source prototype for pump and probe experiments planned at the European XFEL. Tunable IR/THz radiation sources using synchrotron radiation from a dipole magnet, transition radiation, high gain FELs and coherent radiation of tailored or premodulated beams are currently under consideration. This work describes start-to-end simulations for generating the FEL radiation using an APPLE-II undulator with electron beams produced by the PITZ accelerator. Analysis of the physical parameter space has been performed with tools of the FAST program code package. Electron Beam dynamics simulations were performed by using the ASTRA code, while the GENESIS 1.3 code was used to study the SASE process. The results of these studies are presented and discussed in this paper.

INTRODUCTION

The concept of generating IR/THz radiation by electron bunches from a linear accelerator for pump and probe experiments at the European XFEL was presented in Ref. [1]. One of the important requirements for the IR/THz pulse is the possibility for a precise synchronization with the x-ray pulse. A way to meet this requirement is generating the IR/THz pulse from the same type of electron source which serves the European XFEL and therefore can provide the same time structure and repetition rate as those of the x-ray pulses.

The Photo Injector Test facility at DESY, Zeuthen site (PITZ) has been established to develop, study and optimize high brightness electron sources for modern linac-based short-wavelength Free-Electron Lasers (FELs) like FLASH [2] and the European XFEL [3]. The photocathode laser system at PITZ has the essential feature to be able to produce various temporal pulse shapes [4]. The flat-top temporal profile with a FWHM length of 20-22 ps and ~2 ps rise/fall times is usually used for the operation. The electron bunch charge can be varied from a few pC to 4 nC and the beam can be accelerated up to ~22 MeV/c.

Since PITZ serves as the facility for commissioning and optimizing RF guns for the European XFEL [5,6] the same characteristics (time structure and beam quality) of the elec-

tron beam from the RF gun at PITZ is available as it will be at the European XFEL. In addition, the site of a PITZ-like setup is small enough to fit in the experimental hall for the European XFEL users so that the transport of the IR/THz radiation to the user experiments is very short. From these advantages, PITZ can be considered as an ideal machine for the development of a prototype IR/THz source for pump-probe experiments at the European XFEL.

With the current techniques for the production of electron beam at PITZ and different means for radiation generation (dipole magnet, transition radiation, high gain FELs, coherent radiation of tailored or premodulated beams, etc), it will be possible to cover wavelengths in the whole radiation spectrum from IR (μm) to THz (cm) wavelengths with a variety of field patterns (from single-cycled to narrow-band), and with a high level of the peak and average radiation power [1].

As the PITZ beamline has limited possibilities to install additional components, a preliminary layout for the IR/THz radiation source was developed and is presented in Fig. 1. Preliminary studies by using this layout have been done in order to get benchmark results for actual beamline modifications and further studies. The layout consists of a 1.6-cell L-band photo RF gun surrounded by main and bucking solenoids, a cut disk structure (CDS) booster, a c-shape chicane bunch compressor (D1 to D4), quadrupole magnets (Q1 to Q11), screen stations (S1 to S5) and an APPLE-II type undulator [7]. The components and their positions in this layout from the RF gun to the screen S1 are similar to those of the current PITZ layout. With this preliminary layout, we plan to study the radiation generation with 2 procedures: (i) Self-Amplification of Spontaneous Emission Free-Electron Lasers (SASE FELs) in the undulator using an uncompressed, high charge electron bunch and (ii) Coherent Transition Radiation (CTR) using an ultra-short electron bunch which is compressed by the chicane bunch compressor. The SASE radiation is anticipated to cover radiation wavelengths of 20-100 μm while radiation wavelengths above 100 μm are expected from the CTR.

This paper presents start-to-end (S2E) numerical simulations for the SASE FEL radiation in the wavelength range of 20-100 μm . An uncompressed electron beam with 4 nC bunch charge and the APPLE-II type undulator were used in the simulations. Calculation of the saturation characteristics has been performed with tools of the FAST program code package [8-10]. Beam dynamics simulations were performed by using A Space charge TRacking Algorithm (ASTRA) code [11], while the GENESIS1.3 code [12] was used to study the SASE process.

* prach.boonpornprasert@desy.de

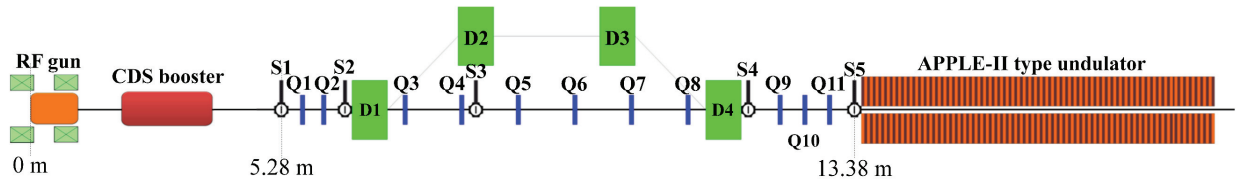


Figure 1: Preliminary schematic layout of the IR/THz facility at PITZ. Here S, Q and D represent screen stations, quadrupole magnets and dipole magnets, respectively.

CONSIDERATIONS OF UNDULATOR PERIOD LENGTH AND ELECTRON BEAM MOMENTUM

The objectives of this section are to determine the undulator period length and the electron beam momentum for generating radiation wavelengths of $20\ \mu\text{m}$ and $100\ \mu\text{m}$. The undulator used in this study is an APPLE-II type undulator in circular polarization mode. Its peak magnetic field (B_0) and undulator parameter (K) can be calculated by using the following equations [13, 14]:

$$B_0 = 1.54 \exp\left(-4.46 \frac{g}{\lambda_u} + 0.43 \left(\frac{g}{\lambda_u}\right)^2\right), \quad (1)$$

$$K = \frac{eB_0\lambda_u}{2\pi m_e c}, \quad (2)$$

where g is the undulator gap, λ_u is the undulator period length, e is the electron charge, m_e is the electron mass and c is speed of light. The goal FEL radiation wavelength (λ_{rad}) can be calculated by the well-known undulator equation:

$$\lambda_{rad} = \frac{\lambda_u}{2\gamma^2} (1 + K^2), \quad (3)$$

where γ is the Lorentz factor of the electron beam.

In order to achieve the shortest FEL saturation length, the shortest period length of the undulator is expected. The minimum gap is chosen to be 10 mm for sufficient space for the beam pipe. In order to avoid strong space-charge effects during the beam transportation, the minimum electron beam momentum is limited to 15 MeV/c and the beam momentum needs to be as high as possible for each radiation wavelength. However, the maximum electron beam momentum is limited at 22 MeV/c which is the practical maximum momentum used at PITZ. Figure 2 presents the calculated beam momentum as a function of the undulator gap for each case of radiation wavelength and undulator period length. Under the above mentioned conditions, the proper period length is 40 mm, from which follows that the radiation wavelengths of $20\ \mu\text{m}$ and $100\ \mu\text{m}$ can be generated with beam momenta of 22 MeV/c and 15 MeV/c, and gap widths of $\sim 16.5\ \text{mm}$ and $\sim 10\ \text{mm}$, respectively.

OVERVIEW OF THE PARAMETER SPACE

An analysis of the parameter space of the SASE FEL at PITZ is performed for two cases of radiation: $100\ \mu\text{m}$ wavelength using a 15 MeV/c electron beam and $20\ \mu\text{m}$ wavelength using a 22 MeV/c electron beam. It is performed

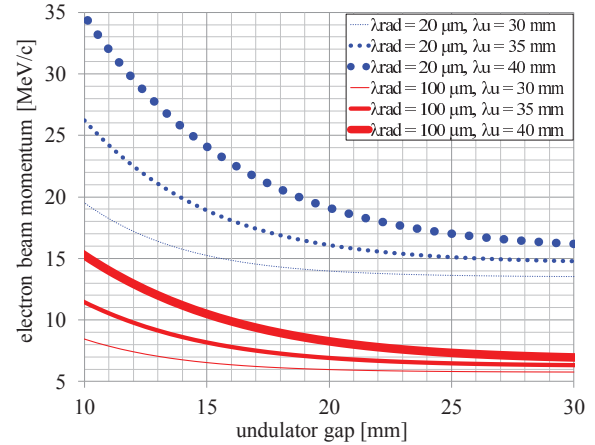


Figure 2: Electron beam momenta for radiation wavelengths of $20\ \mu\text{m}$ and $100\ \mu\text{m}$ as a function of the undulator gap for the different period lengths of the undulator.

by means of tools implemented in the code package FAST [8–10]. We assume natural focusing properties of the helical undulator, thus the remaining parameters of the problem are photon wavelength, energy of the electron beam, peak current, emittance, and energy spread. The numerical solution of the corresponding eigenvalue equation [8, 10] shows that the main physical effects defining the operation of the FEL amplifier are the diffraction effects and the space charge effects. The influence of the longitudinal velocity spread due to emittance and energy spread is negligible.

Figures 3 and 4 show an overview of the saturation characteristics of the SASE FEL versus peak current and emittance. The gray circles at these plots denote the points in the parameter space which we analyze below with detailed numerical simulations with the code GENESIS 1.3. An important feature of the physical parameter space is the small value of the diffraction parameter and the large value of the space charge parameter [8]. In the largest fraction of the parameter space we observe pretty slow dependence of the saturation characteristics on the emittance which reflects the feature of the logarithmic dependence of the FEL gain for small values of the diffraction parameter [8]. At small emittances we see degradation of the FEL gain due to strong space-charge fields. Strong diffraction effects are important also as a factor for a significant reduction of the slippage of the radiation with respect to the kinematic slippage due to the fact that the group velocity of the amplified wave, $\partial\omega/\partial k$,

is less than the velocity of light (c) [8]. This effect allows effective operation of the FEL amplifier driven by short electron pulses. Analysing the influence of the peak current shows that operation at higher currents is more preferable for a reduction of the saturation length and an increase of the peak radiation power. Note that the parameter space of the PITZ FEL is pretty close to that of the first SASE FEL by the UCLA/LANL/RRCKI/SLAC group [8, 15, 16].

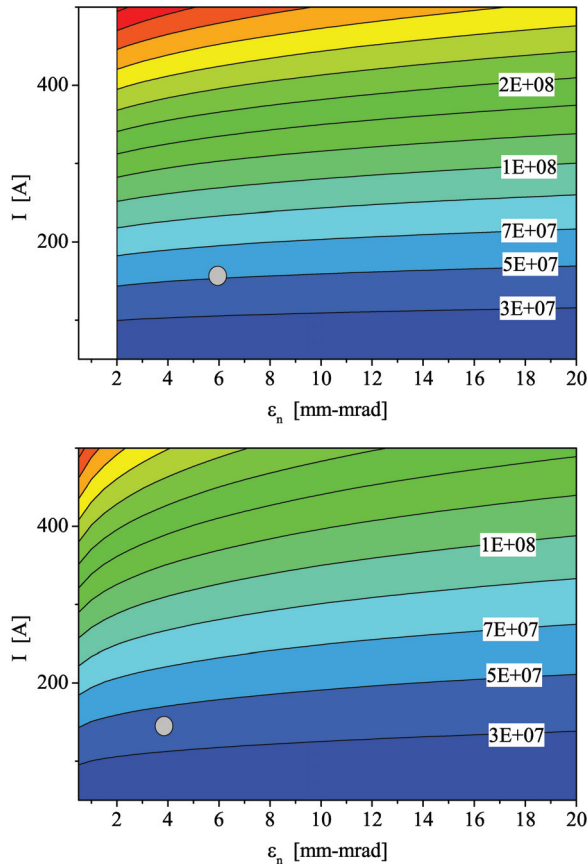


Figure 3: Contour plot for the saturation power [W] versus peak current [A] and emittance [mm-mrad]. Top and bottom plots correspond to the cases of 100 μm using a 15 MeV/c electron beam and 20 μm using a 22 MeV/c electron beam, respectively. The calculations have been performed with the code FAST.

BEAM DYNAMICS SIMULATIONS

Beam dynamics simulations using the ASTRA code were performed in order to deliver an uncompressed 4 nC electron beam from the cathode to the undulator entrance. Space-charge calculations were included in the simulations. The beam transport line layout used in these simulations follows the schematic diagram in Fig. 1. A flat-top cathode laser pulse with a FWHM length of 20 ps and ~ 2 ps rise/fall times was used. In order to ensure that the rms laser spot size is big enough for generating 4 nC bunch charge, the rms laser spot size was set to 1 mm which is close to the maximum size from the practical point of view. The peak electric field

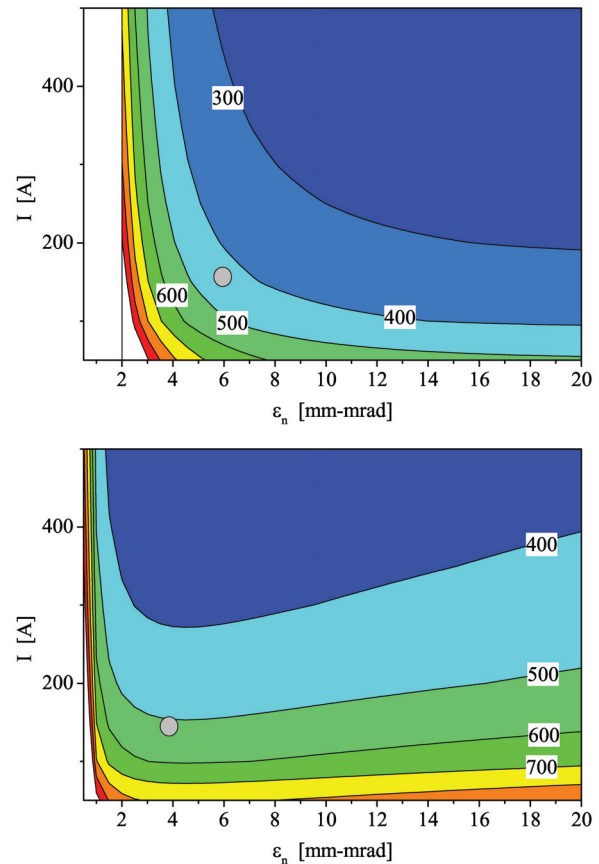


Figure 4: Contour plot for the saturation length [cm] versus peak current [A] and emittance [mm-mrad]. Top and bottom plots correspond to the cases of 100 μm using a 15 MeV/c electron beam and 20 μm using a 22 MeV/c electron beam, respectively. The calculations have been performed with the code FAST.

at the cathode was fixed at 60 MV/m and the booster peak electric fields were set to 10 and 18 MV/m for the beam momenta of 15 MeV/c and 22 MeV/c, respectively.

The contour plots in the previous section indicate that the emittance values at the undulator entrance should be large enough in order to get rid of strong space-charge fields. However, if one realizes beams with high bunch charge and quite low momentum, a huge increase of the emittance during the beam transport can be expected. For this reason, the main solenoid current at the gun was optimized for minimum beam emittance values at the first screen station (S1) for both cases of beam momenta. Figure 5 shows the normalized transverse emittance as a function of the main solenoid current. The minimum emittance values were obtained at the main solenoid current of 388 A and 390 A for the cases of beam momenta of 15 MeV/c and 22 MeV/c, respectively.

Simulations using the optimized main solenoid current were done from the cathode to the undulator entrance. The quadrupole magnets Q1 to Q10 were used for beam transport and matching. The matching strategy is that the transverse size is slightly focused during the transport in order to have a

compromise between the smallest beam size and the weakest beam divergence at the undulator entrance. Figure 6 shows the evolutions of rms beam sizes and the emittance values through the RF gun, the booster cavity and the matching section (S1 to S5). The simulation results show that the growth of emittance in vertical plane is bigger than that of the horizontal plane for both cases of beam momenta. For the case of 15 MeV/c, the emittance growth from the begin to the end of the matching section is about a factor 3 while it is about a factor 2 for the case of 22 MeV/c. The asymmetry of the emittance values between vertical and horizontal planes is due to asymmetric quadrupole focusing strength between two planes [17]. The final transverse parameters and longitudinal profiles of the beams at the undulator entrance are shown in Table 1 and Fig. 7, respectively. Parameters denoted by the gray circles in Fig. 3 and Fig. 4 are illustrated for these final beam profiles. Saturation power of more than 30 MW and a saturation length around 5 m can be expected. The strategies of beam optimization and matching still have to be improved in order to deliver beams which allow for shorter saturation length.

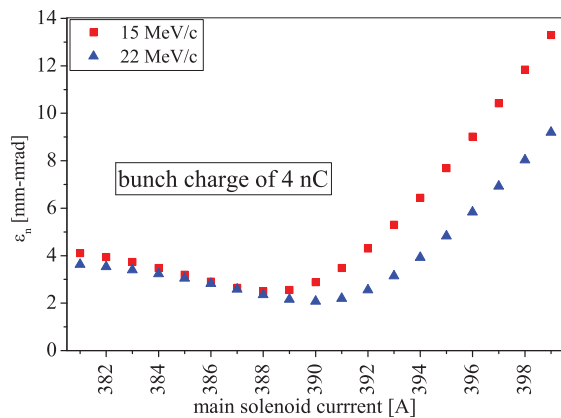


Figure 5: Simulated normalized transverse emittance at the screen S1 as a function of main solenoid current.

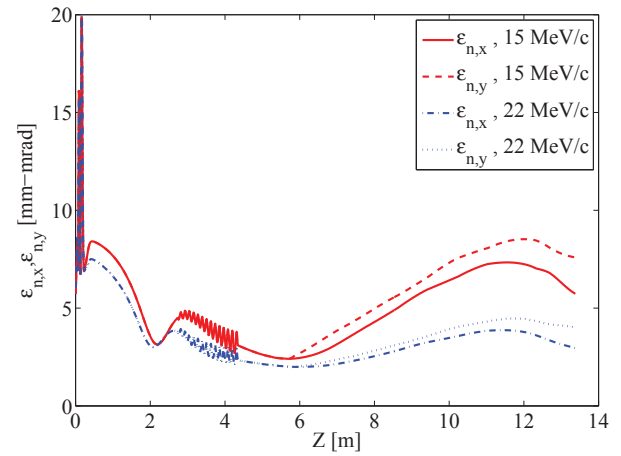
Table 1: Transverse Parameters of the Matched Beams at the Undulator Entrance

Parameters	15 MeV/c	22 MeV/c
σ_x [mm]	0.36	0.25
σ_y [mm]	0.36	0.25
$\epsilon_{n,x}$ [mm-mrad]	6.34	2.95
$\epsilon_{n,y}$ [mm-mrad]	7.16	3.98
α_x	0.62	0.20
α_y	1.36	-0.03

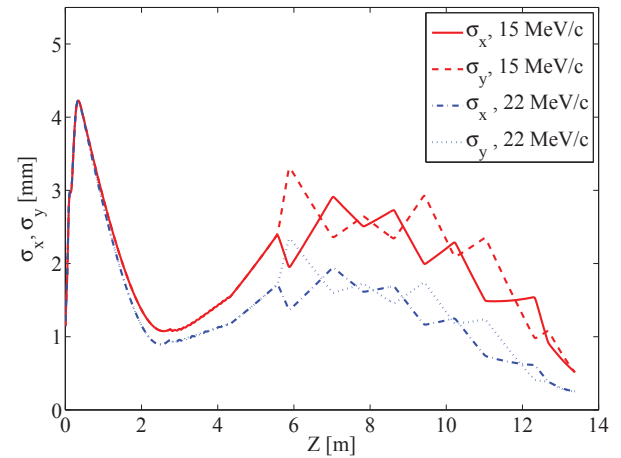
FEL SIMULATIONS

Simulations of the FEL radiation were performed using the GENESIS 1.3 code. The calculations in time-dependent mode including space-charge effects were used in the simulations. The simulations were performed for both cases of radi-

ISBN 978-3-95450-133-5



(a) Normalized transverse emittance.



(b) Transverse rms size.

Figure 6: Evolutions of the transverse emittances ($\epsilon_{n,x}$, $\epsilon_{n,y}$) and transverse rms sizes ($\sigma_{n,x}$, $\sigma_{n,y}$) of the electron beams from the cathode to the undulator entrance.

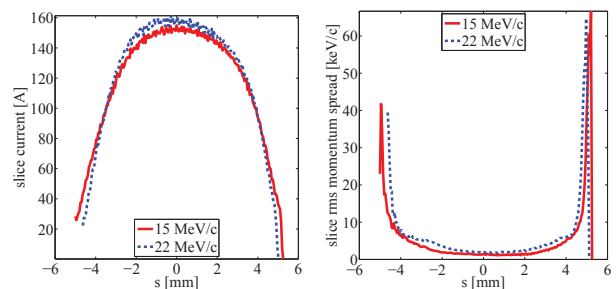


Figure 7: The slice current (left) and the slice rms momentum spread (right) of the matched beams at the undulator entrance.

ation: 20 μm and 100 μm . The matched beams from the previous section were used as the input beams for GENESIS 1.3. The undulator period length was set to 40 mm and the undulator length is assumed to be 7 m (175 periods) in order to be long enough to reach the saturation points for the both cases. In this preliminary simulation, the grid size for the field calculation was set to be larger than the transverse radi-

ation size along the entire undulator length in order to avoid complication of the boundary conditions.

Figure 8 presents the peak power along the undulator. The saturation lengths are 4.12 m (103 periods) and 5.60 m (140 periods) for the radiation wavelengths of 100 and 20 μm , respectively. Figure 9 presents the temporal and spectral structures of the radiation pulses at the points of saturation. For 100 μm , the saturation power is about 90 MW while a spectrum bandwidth of the main peak is about 3 %. For 20 μm , the saturation power is about 130 MW with a bandwidth of the main peak in the spectrum spectrum is less than 1 %. By comparing these results with the results from the code FAST in Fig. 3 and Fig. 4, the saturation lengths from the simulations are corresponding well to the results from those contour plots. In contrast, the saturation powers from the simulations are higher than those in the contour plots for the both cases.

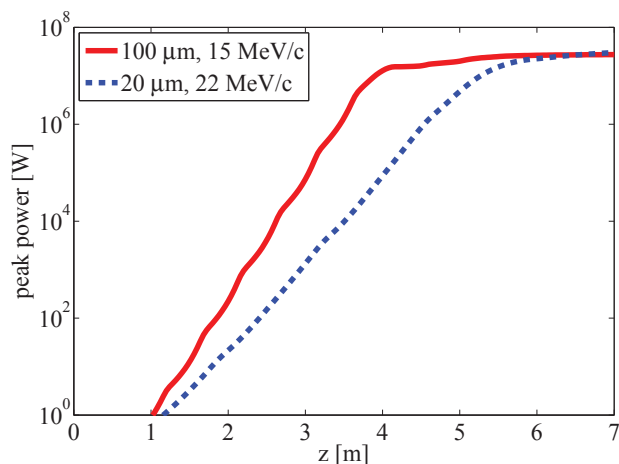
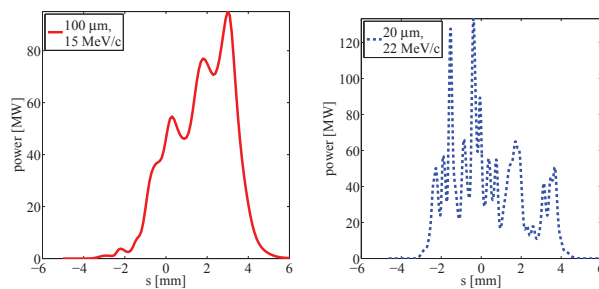


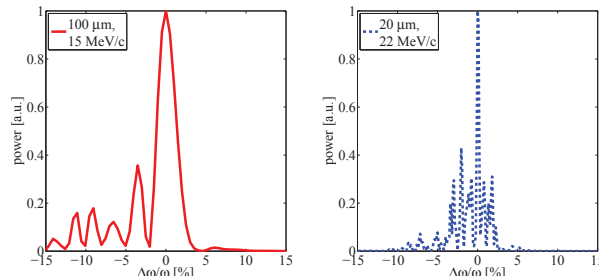
Figure 8: Output peak power along the undulator axis for the cases of 100 μm using a 15 MeV/c electron beam and 20 μm using a 22 MeV/c electron beam.

CONCLUSION AND OUTLOOK

The parameter space of a new IR/THz source based on PITZ setup was studied. Analysis of the physical parameter space was done using the FAST code and preliminary start-to-end simulations of the SASE FEL were performed using the ASTRA and the GENESIS 1.3 codes. The results show that a radiation peak power of more than 90 MW with a narrow bandwidth below 3 % can be achieved. However, the strategies of electron beam optimization and matching still can be improved in order to enhance the FEL performance. In a next step, FEL simulations including waveguide boundary conditions will be studied and performed. Already now this case study shows interesting options for a tunable, synchronized IR/THz source for pump-probe experiment at the European XFEL.



(a) Temporal profiles of the radiation pulses.



(b) Spectral profiles of the radiation pulses.

Figure 9: Temporal and spectral profiles of the radiation pulses at the saturation points. Left and right plots correspond to the case of 100 μm using a 15 MeV/c electron beam and 20 μm using a 22 MeV/c electron beam, respectively.

ACKNOWLEDGMENT

The authors would like to thank colleagues at PITZ for the useful comments and discussions.

REFERENCES

- [1] E. Schneidmiller et al., “Tunable IR/THz source for pump probe experiment at European XFEL”, in *Proc. 34th Int. Free-Electron Laser Conf.*, Nara, Japan, 2012, pp. 503-506.
- [2] W. Ackermann et al., “Operation of a free-electron laser from the extreme ultraviolet to the water window” *Nature Photon.*, vol. 1, pp. 336-342, 2007.
- [3] M. Altarelli et al., “The European x-ray free-electron laser technical design report”, DESY, Hamburg Report No. DESY 2006-097, 2007
- [4] I. Will and G. Klemz, “Generation of flat-top picosecond pulses by coherent pulse stacking in a multicrystal birefringent filter”, *Optics Express*, vol. 16, pp. 14922-14937, 2008.
- [5] I. Isaev et al., “Conditioning status of the first XFEL gun at PITZ”, in *Proc. 35th Int. Free-Electron Laser Conf.*, New York, 2013, pp. 283-286.
- [6] M. Otevreil et al., “Report on gun conditioning activities at PITZ in 2013”, in *Proc. 5th Int. Particle Accelerator Conf.*, Dresden, Germany, 2014, pp. 2962-2964.
- [7] S. Sasaki, “Analyses for a planar variably-polarizing undulator”, *Nucl. Instrum. and Methods A*, vol. 347, pp. 83-86, 1994.
- [8] E.L. Saldin, E.A. Schneidmiller and M.V. Yurkov, *The Physics of Free Electron Lasers*. Berlin, Germany: Springer, 2000.

- [9] E.L. Saldin, E.A. Schneidmiller and M.V. Yurkov, "FAST: a three-dimensional time-dependent FEL simulation code", *Nucl. Instrum. and Methods A*, vol. 429, pp. 233-237, 1999.
- [10] E.L. Saldin, E.A. Schneidmiller and M.V. Yurkov, "The general solution of the eigenvalue problem for a high-gain FEL", *Nucl. Instrum. and Methods A*, 475, pp. 86-91, 2001.
- [11] K. Flöttmann, ASTRA particle tracking code. Available: <http://www.desy.de/~mpyf1o/>.
- [12] S. Reiche, "GENESIS 1.3: a fully 3D time-dependent FEL simulation code", *Nucl. Instrum. and Methods A*, vol. 429, pp. 243-248, 1999.
- [13] C.J. Boccheta et al., "Conceptual Design Report (CDR) for the FERMI@Elettra project", Sincrotrone Trieste, Trieste, ST/F-TN-07/12, 2007.
- [14] P. Schmüser et al., *Ultraviolet and soft x-ray free-electron lasers*, Berlin, Germany: Springer, 2008, pp. 58-59.
- [15] M. Hogan et al., "Measurements of gain larger than 10^5 at $12\ \mu\text{m}$ in a self-amplified spontaneous-emission free-electron laser", *Phys. Rev. Lett.*, vol. 81, pp. 4867-4870, 1998.
- [16] E.L. Saldin, E.A. Schneidmiller and M.V. Yurkov, "Numerical simulations of the UCLA experiments on a high gain SASE FEL", *AIP Conference Proceedings*, vol. 468, 321-333, 1999.
- [17] G. Kourkafas et al., "Emittance increase and matching along the tomography module at PITZ", in *Proc. 5th Int. Particle Accelerator Conf.*, Dresden, Germany, 2014, pp. 1144-1146.